Metallization of the C60/Rh(100) interface revealed by valence photoelectron spectroscopy and density functional theory calculations

Abdou-Ciss Wade, Silvano Lizzit, Luca Petaccia, Andrea Goldoni, Djibril Diop et al.

Citation: J. Chem. Phys. **132**, 234710 (2010); doi: 10.1063/1.3432778

View online: http://dx.doi.org/10.1063/1.3432778

View Table of Contents: http://jcp.aip.org/resource/1/JCPSA6/v132/i23

Published by the American Institute of Physics.

Metallization of the C_{60}/Rh(100) interface revealed by valence photoelectron spectroscopy and density functional theory calculations

Abdou-Ciss Wade,[1,2,a)] Silvano Lizzit,[1] Luca Petaccia,[1] Andrea Goldoni,[1] Djibril Diop,[2] Hande Üstünel,[3,b)] Stefano Fabris,[3,c)] and Stefano Baroni[3]
[1]*Sincrotrone Trieste SCpA, ss 14 km 163, 5 in AREA Science Park, 34149 Trieste, Italy*
[2]*Department of Physics, Cheikh Anta Diop University, BP 5005 Dakar, Senegal*
[3]*CNR-IOM DEMOCRITOS, Theory@Elettra Group, Istituto Officina dei Materiali, ss 14 km 163, 5 in AREA Science Park, 34149 Trieste, Italy and SISSA-Scuola Internazionale Superiore di Studi Avanzati, via Bonomea 265, I-34136 Trieste, Italy*

(Received 10 November 2009; accepted 30 April 2010; published online 21 June 2010)

The electronic structure of single and multiple layers of C_{60} molecules deposited on a Rh(100) surface is investigated by means of valence photoemission spectroscopy and density functional theory calculations. The binding of the fullerene monolayer to the metal surface yields the appearance of a new state in the valence band spectrum crossing the Fermi level. Insight into the metallization of the metal/fullerene interface is provided by the calculated electronic structure that allows us to correlate the measured interface state with a strong hybridization between the Rh metal states and the highest and lowest molecular orbitals. This results in a net charge transfer of $\approx 0.5e-0.6e$ from the metal to the *p* states of the interfacial C atoms. The charge transfer is shown to be very short range, involving only the C atoms bound to the metal. The electronic structure of the second C_{60} layer is already insulating and resembles the one measured for C_{60} multilayers supported by the same substrate or calculated for fullerenes isolated in vacuum. The discussion of the results in the context of other C_{60}/metal systems highlights the distinctive electronic properties of the molecule/metal interface determined by the Rh support. © *2010 American Institute of Physics*. [doi:10.1063/1.3432778]

I. INTRODUCTION

An important scientific challenge in carbon-based materials is the metallization of fullerene layers upon electron doping. It is well known that C_{60} is a strong electron acceptor, and electron doping of C_{60} solids is easily achieved, for example, by intercalation of alkali metals.[1–3] Electron-doped intercalated C_{60} compounds show several phases with distinct properties, among which the most interesting are the metallic and superconducting phases with an excess charge of almost 3 electrons/molecule.[1–10]

The intercalation of dopant atoms is not the only way to form metallic C_{60} systems. The chemisorption of a single layer of C_{60} on metal surfaces, which typically involves hybridization between the molecular orbitals of C_{60} and the metal states near the Fermi level as well as interface charge reorganization, may result in a net charge transfer from the metal to the C_{60} lowest unoccupied molecular orbital (LUMO).[11–18] This mechanism is known to drive the chemisorbed molecular layer into a metallic state only for Cu, Ag, and Au metal surfaces,[11,12,15,16,18,19] while for all the other metallic surfaces investigated so far,[13,14,17,20–24] the metallicity of the overlayer is not clearly proved. This behavior is mainly governed by molecule-substrate interfacial interactions or by specific electronic properties of the substrate. Yet, other noble metal surfaces such as Rh (Refs. 20 and 21) and Pt (Refs. 19 and 22) should give a clear metallic character to the C_{60} overlayer, but the reported experimental evidence seems to exclude these substrates[19,22] or does not provide a clear conclusion.[20,21]

For Rh, in particular, the observed changes in the work function upon chemisorption of 1 ML of C_{60} on Rh(111)[20,21] suggested that the hybridization of Rh *d*-states with the highest occupied molecular orbital (HOMO) is more effective than the hybridization with the LUMO, resulting in a net delocalization of electrons from C_{60} to the Rh surface. However, no new photoemission states were observed near the Fermi level, while the presence of a $t_{1u} \rightarrow t_{1g}$ (LUMO $\rightarrow$ LUMO+1) transition was reported in the electron energy loss spectra, suggesting indeed that some electrons were instead populating the LUMO (t_{1u}) orbitals.[21]

In the present work, we investigate, by means of valence band photoemission spectroscopy and density functional theory (DFT) calculations, the electronic structure of C_{60} molecules deposited onto a Rh(100) surface. The valence band spectra show the appearance of a new state at the Fermi level, which calculations reveal to be a hybrid Rh–C_{60} state. This state has a significant component over the molecular LUMO state, resulting in a net charge transfer from the Rh substrate to C_{60} and giving thus a metallic character to the C_{60} monolayer.

This paper is organized as follows: the details of the

[a)]Present address: Physics Department, Cheikh Anta Diop University, BP 5005 Dakar, Senegal.
[b)]Present address: Department of Physics, Middle East Technical University, Ankara 06531, Turkey.
[c)]Author to whom correspondence should be addressed. Electronic mail: fabris@sissa.it.

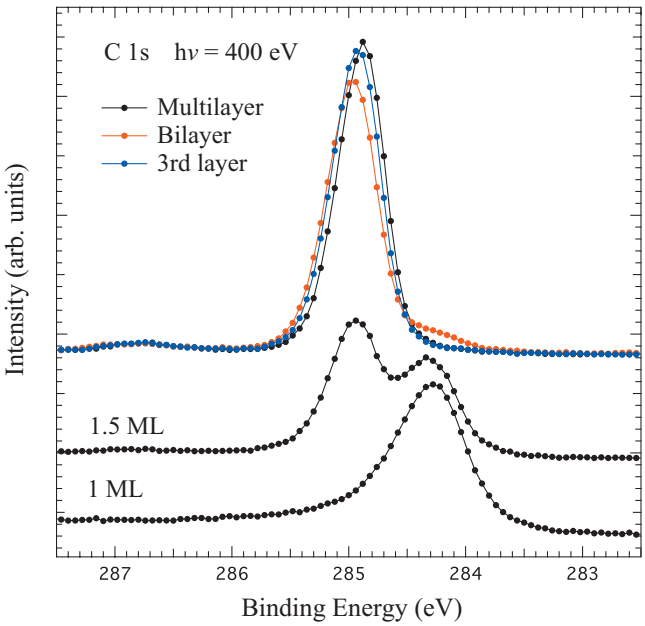

FIG. 1. C 1*s* core level spectra obtained during TD of a C_{60} multilayer. Some selected spectra are reported.

photoemission measurements and of the DFT calculations are described in Sec. II. Our results are then reported and discussed in Sec. III by considering first a single monolayer of C_{60} adsorbed on Rh(100) (Sec. III A) and then a molecular bilayer on the same metal surface (Sec. III B). The main findings are finally summarized in Sec. IV.

II. METHODS

A. Experimental measurements

The measurements were performed in the ultrahigh vacuum experimental chamber (base pressure of about 10^{-10} mbar) of the SuperESCA beamline at the Elettra Synchrotron. Valence band photoemission data were recorded with a double-pass hemispherical electron energy analyzer at normal emission using photon energies of 140 and 70 eV with an overall energy resolution of about 80 meV. The binding energy values are defined with respect to the Fermi level (E_F) of the clean Rh(100) substrate. The Rh(100) substrate was cleaned by cycles of Ar^+ sputtering and high temperature annealing in oxygen and hydrogen atmosphere. C_{60} was evaporated from a degassed tantalum crucible and deposited on the clean rhodium substrate kept at 400 K to form the multilayer. The thickness of the multilayer was 10 ± 1 ML. The formation of the monolayer is carried out either by thermal desorption (TD) of the deposited multilayer by annealing the film above 550 K or by depositing C_{60} with the substrate kept at 600 K.[18,22] Here we used both techniques. The formation of a second layer above the monolayer was obtained by TD of the multilayer following the C 1*s* core level (Fig. 1) or by depositing another layer above the monolayer. In both cases, we know that we have not formed the third layer (because the core level is shifted and the valence band is insulating like the multilayer) and that the amount of C_{60} is more than 1.5 ML (see Fig. 1).

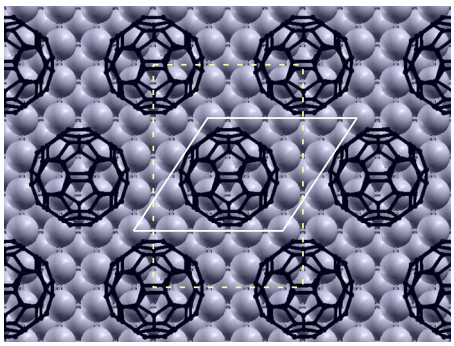

FIG. 2. Top view of the C_{60} monolayer adsorbed on the Rh(100) surface. The vectors defining the computational supercell are marked by white solid lines. Carbon and rhodium atoms are represented by black and gray spheres, respectively.

B. Numerical simulations

DFT calculations were performed with the Perdew–Burke–Ernzerhof[25] exchange-correlation functional in a plane-wave pseuopotential framework, as implemented in the PWscf code of the QUANTUM ESPRESSO distribution,[26,27] using ultrasoft pseudopotentials.[28,29] The C_{60} monolayer adsorbed on the Rh(100) surface was simulated in a $c(4\times6)$ periodic arrangement (see dashed lines in Fig. 2) by using the supercell displayed in Fig. 2 (solid lines). In the absence of low energy electron diffraction (LEED) data for this specific system, we modeled a coherent interface between the squared lattice of the Rh(100) surface and a monolayer of C_{60} molecules in a hexagonal arrangement (slightly distorted to yield commensurability). The periodicity was set such that the average C_{60}–C_{60} intermolecular distance (10.4 Å) was as close as possible to the corresponding experimental value in the hexagonal C_{60} arrangement along the (111) planes of a fcc fullerene crystal (10.1 Å). We stress, however, that due to the weakness of intermolecular interactions, the main conclusions of our study do not depend on this specific periodicity of the model structure. Three- and four-layer Rh slabs were used as simplified models for the Rh(100) surface with the calculated equilibrium bulk lattice parameter of 3.85 Å. In the resulting distorted hexagonal symmetry of the monolayer, the shorter distances between two neighboring C_{60} molecules are 9.81 and 10.92 Å. Opposite surfaces of adjacent supporting metal slabs were separated by more than 16.5 Å, leaving more than 8 Å between the top of the adsorbed C_{60} molecule and the periodic image of the metal surface above it. Brillouin zone integrations for metallic structures were performed on a (4×4) Monkhorst–Pack grid consisting of 10 points (including Γ) and with a Methfessel–Paxton[30] smearing of 0.01 Ry. Isolated fullerene molecules were simulated by sampling electronic states only at the Γ point. In the case of the adsorbed monolayer, all atomic positions were relaxed according to the Hellmann–Feynman forces, except for the two lowermost Rh layers whose distance was kept fixed to the bulk value. In addition to a single layer of C_{60} molecules, the effects of a second layer were also investigated. In this case, the C_{60} molecules on the top layer were arranged above hollow sites left between the arrangements of C_{60} molecules on the bottom layer, with one of the hexagons facing downward. A

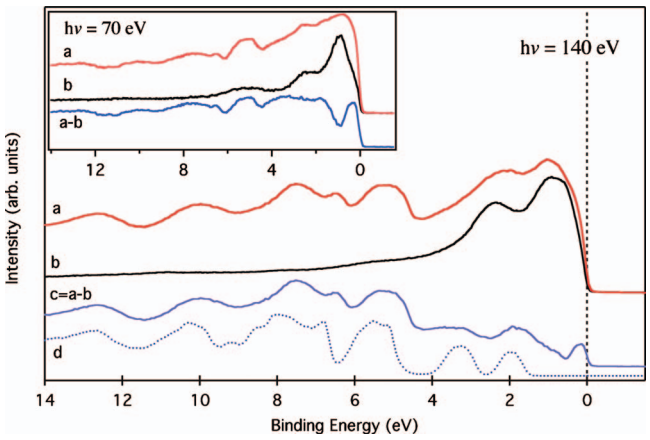

FIG. 3. Valence band photoemission spectra of (a) 1 ML of C_{60} on Rh(100), (b) a clean Rh(100) surface (reduced by a factor of 4.5, see text for details) and (d) a C_{60} multilayer. The spectrum (c) is obtained by the difference between spectra (a) and (b). All these spectra are measured with a photon energy of 140 eV. Inset: the same spectra described above obtained with a photon energy of 70 eV. Here, an attenuation factor of 6.0 (see text for details) was used for the spectra difference (c).

vertical distance of 1.5 Å was set between the two layers. In this case, the vacuum region between the topmost atoms of the second-layer C_{60} molecules and the bottom of the next Rh surface slab was increased to 12 Å. No further structural relaxation was performed for the bilayer system.

III. RESULTS AND DISCUSSION

A. C_{60} monolayer on Rh(100)

1. Photoemission data: Interface electronic states

Figure 3 shows the valence band photoemission spectra of (a) 1 ML-C_{60}/Rh(100), (b) of the clean Rh(100) surface, and (d) of a C_{60} multilayer film, all obtained with a photon energy of 140 eV. The monolayer spectrum is dominated by the characteristic C_{60} molecular orbitals for binding energies higher than 4 eV, while at lower binding energy, i.e., from the HOMO−1 down to the Fermi level, the major contributions rely upon the emission from Rh 4*d* states. First we note that as observed in other C_{60} monolayer systems on metals, there is a nonrigid shift of the C_{60}-related peaks toward lower binding energies with respect to the multilayer, but the line shape of these peaks is only slightly modified compared to the multilayer. The shift is mainly due to a better screening of the on-site electron-electron correlation energy in the monolayer given by the close proximity to the metallic surface underneath.[31] Since the line shape of the C_{60} peaks is not heavily modified, this indicates that the molecules are still intact and not distorted after the adsorption process.

In addition, we note from Fig. 3 that the spectral intensity of the band edge near the Fermi level is higher for the monolayer than for the clean Rh(100). This is a clear sign of the presence of new states near E_F. In order to extract the structures of the overlayer and to make the presence of new states near E_F more evident, as well as to resolve other new features related to the interaction between C_{60} and Rh, we have subtracted the clean Rh(100) spectrum from the monolayer spectrum [Fig. 3(c)]. The difference spectrum, displayed in Fig. 3(c), is obtained by subtracting the Rh(100) signal reduced by a factor 4.5 (assuming an inelastic mean free path for photoelectrons of ~5.3 Å in the range of 120–135 eV of the kinetic energy and an overlayer thickness of 8 Å). This is consistent with previous works, suggesting that the photoemission intensity of the substrate in C_{60}/Rh(100) should be attenuated by factors ranging from 3 to 6 with respect to the clean Rh(100) signal.[32] We note that similar results were obtained by repeating the same procedure for different values of the attenuation factor in this range of values.

The difference spectrum displayed in Fig. 3(c) clearly shows the peaks due to the HOMO and HOMO−1 states, which are broadened with respect to the corresponding ones in the multilayer case. Similar broadening and splitting of the HOMO states was observed on the monolayer adsorbed on Al surfaces[13] and Ge(111),[33] where the molecular bonding is expected to be mainly covalent. On these surfaces, the C_{60} monolayer is insulating. In the case of Rh(100), additional features are present between the HOMO and E_F, where a new sharp peak appears. In order to confirm that this peak at E_F is not an artifact of the experimental setup (for example, resulting from a misalignment of the spectra due to instabilities of the photon energy beam), we show in the inset of Fig. 3 the same spectra measured with a different photon energy, i.e., 70 eV. In this case, the attenuation factor of the clean Rh(100) has been chosen to be 6, which corresponds to the assumption of an inelastic mean free path for photoelectrons of 4.8 Å. One can see that the peak at the Fermi level is visible also in this case and the other peaks are the same as obtained at 140 eV. We note that in this case the C_{60} features are suppressed because of the increased weight of the Rh character in the hybrid states due to reasons related to photoemission cross section.[34] This indicates that the C_{60} and Rh states are strongly hybridized, in particular, for binding energies between E_F and 5 eV, where the Rh *d* bands superimpose to the HOMO and HOMO−1 states. Since the Rh 4*d* bands are known to extend a few eV above E_F, similar hybridization is also expected for the LUMO and LUMO+1 C_{60} orbitals.

The new feature at E_F may have different origins. The increase in the peak intensity reducing the photon energy indicates that the interface state at E_F has a strong Rh contribution due to cross section effects and we cannot exclude the possibility that this feature originates exclusively from Rh states without any molecular contribution (in this case, the C_{60} monolayer would be an insulator). According to this interpretation, the C_{60} overlayer would simply act as a momentum scatterer for the Rh photoemitted electrons, averaging the states inside the Brillouin zone. This scenario would then lead to an increase in the density of states (DOS) at E_F in the Γ point, hence compatible with our spectra at normal emission. Instead, the electronic structure calculations described in the following support another interpretation. They provide evidence that the peak at the Fermi level originates from a charge transfer from the metal to the molecular states, leading to a metallization of the interface.

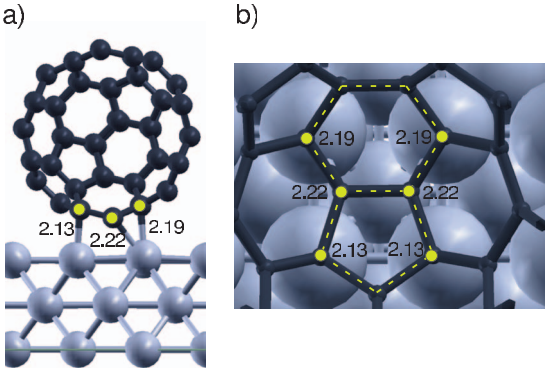

FIG. 4. (a) Side view of the minimum-energy adsorption geometry predicted by the DFT calculations. Yellow circles denote the interfacial C atoms bound to the Rh surface and the lengths of the corresponding bonds are expressed in Å. (b) Magnified view of the local geometric arrangement at the interface. The dashed yellow lines mark the fullerene pentagon and hexagon closest to the metal surface.

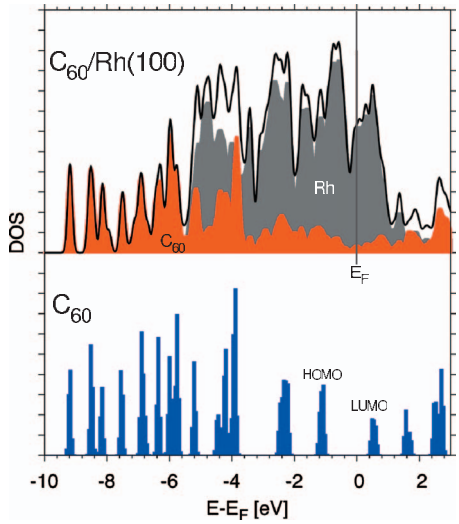

FIG. 5. Top: total DOS (black line) for the 1 ML C_{60}/Rh(100) system and its breakdown into Rh (gray area) and C (red area) contributions calculated by projecting the density on atomic orbitals. Bottom: DOS for a fullerene molecule isolated in vacuum.

2. DFT calculations: Geometry optimization and energetics of adsorption

The equilibrium adsorption geometry was determined by a two step procedure. We first performed a series of single point total-energy calculations without geometric optimization in which C_{60} was positioned at a vertical height of 2 Å above the metal surface. The energy landscape was explored as a function of molecular lateral translations and rotations. In particular, we explored the high-symmetry configurations obtained by placing the molecule on the metal substrate with one of its hexagon, pentagon, or hexagon-pentagon edge facing either the hollow, top, or bridge sites of the Rh(100) square lattice. In addition, for each of these configurations, we also considered rotations of the molecule around its axis perpendicular to the surface through a series of high-symmetry angles. The lowest-energy structure was then fully relaxed. During the structural optimization, the molecule approached the surface decreasing the vertical distance to 1.7 Å (calculated between the center of the closest C atom and the interfacial Rh atom).

The resulting lowest-energy adsorption geometry is displayed in Fig. 4. In this configuration, a pentagon-hexagon edge of C_{60} is oriented parallel to one of the [001] directions of the Rh surface and is in the middle of a surface square, on top of a second-layer Rh atom. The relevant C–Rh bond lengths are displayed in Fig. 4(a), where the interfacial hexagon and pentagon of the fullerene are highlighted by dashed yellow lines and the six C atoms bound to the metal surface are marked by yellow circles. The Rh atoms close to the contact area display very small displacements ≤ 0.1 Å with respect to the equilibrium positions, while the position of the remaining metal atoms is unaffected by C_{60} adsorption.

The molecule/metal distance predicted by the DFT calculations (1.7 Å) is much shorter than the corresponding distance obtained for the adsorption of C_{60} on other transition metal surfaces: 2.4 Å for C_{60}/Ag(111),[35] 2.5 Å for C_{60}/Au(111),[35] or 2.5 Å for C_{60}/Ag(100) (estimated from Fig. 6 of Ref. 35). The latter comparison indicates that the short molecule-metal distance in the present C_{60}/Rh(100) system is not a result of the specific geometry of the (100) surface but is due to the nature of the Rh metal, in particular, the low value of the work function and the extension of the *d* band across the HOMO and LUMO. In order to give further evidence to this fact, we have performed a parallel study on a C_{60} monolayer adsorbed on a Au(100) surface, whose *d* band is ≈ 2 eV below the LUMO. In this case, we obtained a much larger distance of 2.8 Å, compatible with the value reported for the Au(111) surface.[35]

The short molecule/metal distance in the C_{60}/Rh(100) system results in a strong metal-molecule interaction, in analogy with the C_{60}/Rh(111) case[20,21] and actually observed here using TD spectroscopy (results not shown[36]). Indeed, a large adsorption energy of 3.62 eV/molecule is estimated from the total energy difference defined as $E_{C_{60}/Rh(100)} - (E^{ML}_{C_{60}} + E_{Rh(100)})$, where $E_{C_{60}/Rh(100)}$, $E^{ML}_{C_{60}}$, and $E_{Rh(100)}$ are the total energies of the C_{60} monolayer adsorbed on the Rh(100) surface, the C_{60} monolayer isolated in vacuum, and the Rh(100) clean surface, respectively, calculated in the same simulation supercell.

3. DFT calculations: Electronic structure and interface metallization

The total DOS for a single C_{60} monolayer adsorbed on Rh(100) is shown in Fig. 5 (solid black line in the upper panel) together with its decomposition into partial contributions from the Rh and C atoms (displayed in Fig. 5 as gray and red areas, respectively). The latter was obtained by projecting the self-consistent DOS onto the corresponding atomic orbitals (PDOS denotes projected DOS). For reference, the energy of the molecular states for an isolated fullerene molecule is also shown in the lower panel of Fig. 5 (blue areas). Energies are referred to the Fermi energy of the C_{60}/Rh(100) system, while, in order to facilitate the fingerprinting of the peaks, the energies of the molecular states for the isolated fullerene are shifted so as to align with the corresponding ones in the C_{60}/Rh(100) system. We remark that the calculated HOMO and LUMO gap of the C_{60} is under-

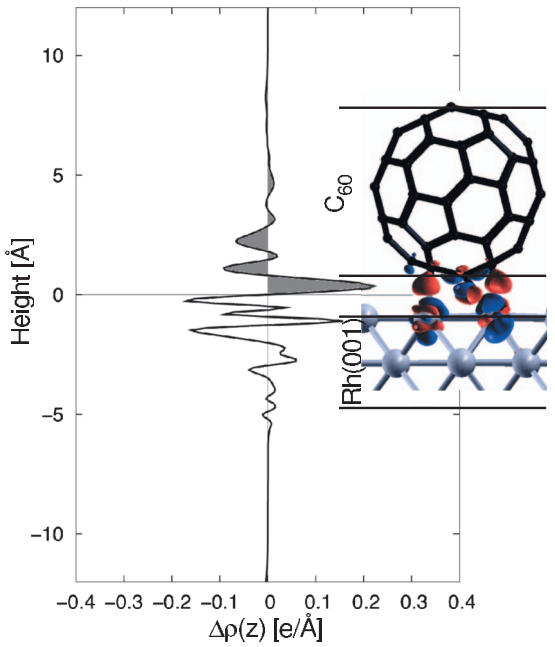

FIG. 6. Differential charge density $\Delta\rho$ (in $e/\text{Å}$) integrated in the xy planes parallel to the C_{60}–Rh interface as a function of the distance (z, in Å) along the direction normal to the surface. Positive/negative values denote charge accumulation/depletion. Horizontal lines limit the extension of the C_{60} molecule and of the Rh(100) metal slab. The inset shows the spatial representation of the charge density redistribution plotted for a value of $|0.04|e/\text{Å}^3$. Positive and negative values are represented by red and blue isosurfaces, respectively.

estimated by 0.7–0.8 eV, in agreement with previous DFT calculations performed with a similar functional.[37,38]

The comparison between the Carbon PDOS of the isolated (blue area in Fig. 5) and supported (red area) fullerenes shows that the interaction with the metal surface strongly modifies the occupied HOMO and HOMO−1 as well as the LUMO and LUMO+1, while the remaining states are weakly perturbed upon adsorption. The position of the Fermi energy is pinned by the metallic surface and falls within the Rh d band (gray area). The C-PDOS of the supported C_{60} monolayer (red area) clearly shows the presence of a continuum of states between the HOMO and LUMO, with a clear peak at E_F as observed in the experimental spectra, hence proving the metallization of the metal/molecule interface. The corresponding molecular states are shown in Fig. 6. These states are strongly hybridized with the underlying Rh metal states and can be directly correlated with the strong molecular binding to the metal surface discussed above.

The formation of interfacial Rh–C bonds results from a transfer of charge from the Rh surface to the interfacial C atoms of the fullerene. A Löwdin charge analysis[39] shows that with respect to a gas phase fullerene, there is a substantial increase in the charge only on the six C atoms that are bound to the Rh surface: $+0.10e$ on the two atoms forming the edge between the interfacial hexagon and pentagon, $+0.09e$ on the two atoms of the hexagon, and $+0.07e$ on the two atoms of the pentagon. Variations in the Löwdin charge on all other C atoms are smaller than $0.02e$. Overall, a charge transfer of $\approx 0.6e$ can be estimated from differences in the

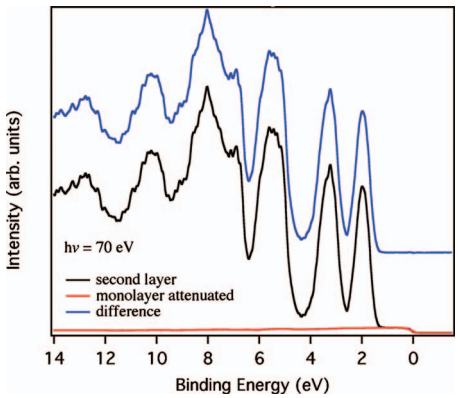

FIG. 7. Valence band photoemission of a C_{60} bilayer (black), a C_{60} monolayer attenuated by a factor of 6 (red), and the difference spectrum (blue).

Löwdin charges of the C and Rh atoms with respect to the corresponding values in the isolated C_{60} molecules and clean Rh(100) surfaces.

The electron density difference and the differential charge density integrated in the xy planes parallel to the interface are displayed in Fig. 6. Positive/negative values (red/blue areas) indicate charge accumulation/depletion. The charge difference is calculated with respect to the sum of the electron distributions of the isolated 1ML C_{60} system and of the Rh(100) metal slab. Horizontal lines indicate the positions of the metal slab and of the fullerene. This analysis provides further evidence of the charge transfer from the metal to the interfacial C atoms, showing that this charge transfer process involves mostly the atoms in the contact region, with a minor contribution from the second layers of Rh and C atoms. An alternative measure of the total charge transfer from the metal to the molecule can be obtained by evaluating the integral highlighted by the gray area in Fig. 6, resulting in $0.5e$.

B. C_{60} bilayer on Rh(100)

The analysis of a double layer system allows us to prove the metallization of the fullerene/Rh interface also in the presence of thicker molecular multilayers. As in other metallic systems,[40] we demonstrate that the C_{60}/Rh(100) interface mainly affects the electronic properties of the first layer only. The valence photoemission spectrum of 2 ML C_{60}/Rh(100) is shown in Fig. 7 (black solid line). By considering the attenuation factor of the signal due to the electron escape depth,[32] the contribution from the first layer should be reduced by a factor of ≈ 6 with respect to the one of the outermost molecules, while the signal from the Rh substrate should be attenuated by a factor of ≈ 36 and therefore almost negligible. Indeed, the spectrum coming from the bilayer system shows a small spectral intensity at E_F, which, according to Fig. 7, is due to the attenuated emission of the first C_{60} layer. The first layer is therefore confirmed to be metallic independent of the presence of other fullerenes above it. Given the high attenuation factor, the metallic signal from the metal/molecule interface is already lost with increasing

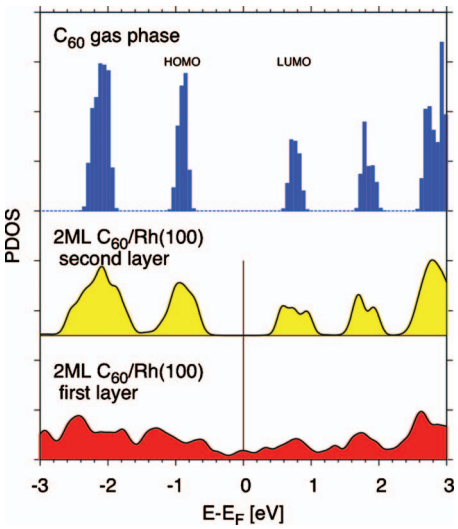

FIG. 8. Energy levels of the molecular orbitals for a C_{60} molecule isolated in vacuum (top). PDOS for the C atoms of a bilayer (middle) of C_{60} adsorbed on the Rh(100) surface (bottom). The PDOS of the two C_{60} layers are plotted separately for the first layer (red area) in contact with the metal surface and for the second layer (yellow area).

number of layers. The subtraction reported in Fig. 7 indicates that the spectrum of the second C_{60} layer is insulating like the multilayer spectrum.

In agreement with the experimental findings, our DFT calculations indicate that C_{60} layers in a multilayer arrangement adsorbed on the Rh(100) surface display an insulating behavior starting from the second layer. The PDOS projected over carbon atoms of the first and the second C_{60} layers are displayed in Fig. 8, together with the reference molecular states for an isolated fullerene molecule (blue area). The Fermi level of the bilayer system is pinned by the charge transfer at the C_{60}/metal interface of the first layer, which displays the same metallic character and charge transfer behavior discussed for the monolayer case. As discussed above, we notice that even though the first monolayer displays a metallic character, the PDOS of the second layer is already insulating and its PDOS shows the characteristic HOMO-LUMO gap of the isolated C_{60} molecule. This analysis clearly demonstrates the short-range character of the surface effects on the deposited C_{60} layers.

IV. CONCLUSIONS

This work emphasizes the role of molecular charge transfer in the ground state of the electronic structure of 1 ML of C_{60} on Rh(100), a case of mainly covalent bonding similar to the Al surfaces. The metallization of the system obtained by adsorbing C_{60} molecules on the Rh(100) surface is demonstrated by valence photoemission experiments combined with DFT calculations. The measured spectra for the 1 ML case show the presence of a new peak crossing the Fermi level. The analysis of the calculated electronic structure reveals that the metallic nature of the system is due to a charge transfer of $\approx 0.5e-0.6e$ from the metal to the p states of the interfacial C atoms, which are strongly hybridized with the underlying Rh atoms. This yields to a metal-molecule distance and to a calculated binding energy of 1.7 Å and 3.4 eV, respectively. The characteristic strong bonding of fullerenes to the Rh metal surface is evident by comparing these values to other C_{60}/metal systems. We note that, from our calculations, this strong bonding is achieved in the absence of surface reconstructions or defects below the adsorbed fullerene, which are typically essential for the chemisorbtion of C_{60} on other noble metals, such as Au (Ref. 41) or Pt.[42]

The analysis of a bilayer system in which 2 ML of C_{60} were adsorbed on the Rh(100) surface allow us to conclude that the same metallization discussed above involves only the first molecular layer. Both the experimental and theoretical analysis shows that the electronic structure of the second layer is already insulating and weakly perturbed with respect to the spectra of the metal-supported C_{60} multilayers.

ACKNOWLEDGMENTS

The present work was supported by the Regione Friuli Venezia Giulia with the project NANOCAT and AMBIOSEN and by the CNR under EUROCORES/FANAS/AFRI. A.-C.W. would like to acknowledge the financial support by ICTP through the STEP fellowship.

[1] O. Gunnarsson, *Alkali-Doped Fullerides: Narrow-Band Solids with Unusual Properties* (World Scientific, Singapore, 2004).
[2] R. C. Haddon, A. F. Hebard, M. J. Rosseinsky, D. W. Murphy, S. J. Duclos, K. B. Lyons, B. Miller, J. M. Rosamilia, R. M. Fleming, A. R. Kortan, S. H. Glarum, A. V. Makhija, A. J. Muller, R. H. Eick, S. M. Zahurak, R. Tycko, G. Dabbagh, and F. A. Thiel, Nature (London) **350**, 320 (1991).
[3] A. F. Hebard, M. J. Rosseinsky, R. C. Haddon, D. W. Murphy, S. H. Glarum, T. T. M. Palstra, A. P. Ramirez, and A. R. Kortan, Nature (London) **350**, 600 (1991).
[4] K. Prassides, Curr. Opin. Solid State Mater. Sci. **2**, 433 (1997).
[5] M. J. Rosseinsky, Chem. Mater. **10**, 2665 (1998).
[6] O. Gunnarsson, Rev. Mod. Phys. **69**, 575 (1997).
[7] T. Yildirim, O. Zhou, and J. E. Fischer, in *The Physics of Fullerene-Based and Fullerene-Related Materials*, edited by W. Andreoni (Kluwer-Academic, Dordrecht, 2000), p. 23.
[8] P. Durand, G. Darling, Y. Dubitsky, A. Zaopo, and M. J. Rosseinsky, Nature Mater. **2**, 605 (2003).
[9] R. W. Lof, M. A. van Veenendaal, B. Koopmans, A. Heessels, H. Jonkman, and G. A. Sawatzky, Int. J. Mod. Phys. B **6**, 3915 (1992).
[10] Y. Iwasa and T. Takenobu, J. Phys.: Condens. Matter **15**, R495 (2003).
[11] S. Modesti, S. Cerasari, and P. Rudolf, Phys. Rev. Lett. **71**, 2469 (1993).
[12] A. J. Maxwell, P. A. Bruhwiler, A. Nilsson, N. Martensson, and P. Rudolf, Phys. Rev. B **49**, 10717 (1994).
[13] A. J. Maxwell, P. A. Brühwiler, D. Arvanitis, J. Hasselström, M. K.-J. Johansson, and N. Mårtensson, Phys. Rev. B **57**, 7312 (1998).
[14] G. K. Wertheim and D. N. E. Buchanan, Solid State Commun. **88**, 97 (1993).
[15] M. R. C. Hunt, S. Modesti, P. Rudolf, and R. E. Palmer, Phys. Rev. B **51**, 10039 (1995).
[16] L. H. Tjeng, R. Hesper, A. C. L. Heessels, A. Heeres, H. T. Jonkman, and G. A. Sawatzky, Solid State Commun. **103**, 31 (1997).
[17] N. Swami, H. He, and B. E. Koel, Surf. Sci. **425**, 141 (1999).
[18] A. Goldoni and G. Paolucci, Surf. Sci. **437**, 353 (1999).
[19] M. Pedio, M. L. Grilli, C. Ottaviani, M. Capozi, C. Quaresima, P. Perfetti, P. A. Thiry, R. Caudano, and P. Rudolf, J. Electron Spectrosc. Relat. Phenom. **76**, 405 (1995).
[20] L. Q. Jiang and B. E. Koel, Phys. Rev. Lett. **72**, 140 (1994).
[21] A. Sellidj and B. E. Koel, J. Phys. Chem. **97**, 10076 (1993).
[22] C. Cepek, A. Goldoni, and S. Modesti, Phys. Rev. B **53**, 7466 (1996).
[23] J. Schiessling, M. Stener, T. Balasubramanian, L. Kjeldgaard, P. Decleva, J. Nordgren, and P. A. Brühwiler, J. Phys.: Condens. Matter **16**, L407 (2004).
[24] A. J. Maxwell, P. A. Brühwiler, S. Andersson, D. Arvanitis, B. Hernnäs, O. Karis, D. C. Mancini, N. Mårtensson, S. M. Gray, M. K.-J. Johansson, and L. S. O. Johansson, Phys. Rev. B **52**, R5546 (1995).

[25] J. P. Perdew, K. Burke, and M. Ernzerhof, Phys. Rev. Lett. **77**, 3865 (1996).
[26] S. Scandolo, P. Giannozzi, C. Cavazzoni, S. de Gironcoli, A. Pasquarello, and S. Baroni, Z. Kristallogr. **220**, 574 (2005).
[27] P. Giannozzi, S. Baroni, N. Bonini, M. Calandra, R. Car, C. Cavazzoni, D. Ceresoli, G. L. Chiarotti, M. Cococcioni, I. Dabo, A. Dal Corso, S. de Gironcoli, S. Fabris, G. Fratesi, R. Gebauer, U. Gerstmann, C. Gougoussis, A. Kokalj, M. Lazzeri, L. Martin-Samos, N. Marzari, F. Mauri, R. Mazzarello, S. Paolini, A. Pasquarello, L. Paulatto, C. Sbraccia, S. Scandolo, G. Sclauzero, A. P. Seitsonen, A. Smogunov, P. Umari, and R. M. Wentzcovitch, J. Phys.: Condens. Matter **21**, 395502 (2009); see http://www.quantum-espresso.org.
[28] D. Vanderbilt, Phys. Rev. B **41**, 7892 (1990).
[29] Pseudopotentials C.pbe-van_bm.UPF and Rh.pbe-nd-rrkjus.UPF from the QUANTUM ESPRESSO distribution were used to describe the electron-ion interaction. The plane-wave basis set and the Fourier components of the electron charge density were limited by energy cutoffs of 30 and 300 Ry, respectively.
[30] M. Methfessel and A. T. Paxton, Phys. Rev. B **40**, 3616 (1989).
[31] R. Hesper, L. H. Tjeng, and G. A. Sawatzky, Europhys. Lett. **40**, 177 (1997).
[32] A. Goldoni, L. Sangaletti, F. Parmigiani, G. Comelli, and G. Paolucci, Phys. Rev. Lett. **87**, 076401 (2001).
[33] A. Goldoni, C. Cepek, M. De Seta, J. Avila, M. C. Asensio, and M. Sancrotti, Phys. Rev. B **61**, 10411 (2000).
[34] J. J. Yeh and I. Lindau, At. Data Nucl. Data Tables **32**, 1 (1985).
[35] L.-L. Wang and H.-P. Cheng, Phys. Rev. B **69**, 165417 (2004).
[36] A.-C. Wade *et al.*, "Thermal stability of C_{60} on Rh(100) measured by fast core level photoemission," J. Chem. Phys. (to be published).
[37] K. Kobayashi and N. Kutita, Phys. Rev. Lett. **70**, 3542 (1993).
[38] S. Hamel, V. Timoshevskii, and M. Cote, Phys. Rev. Lett. **95**, 146403 (2005).
[39] P.-O. Löwdin, J. Chem. Phys. **21**, 374 (1953).
[40] M. R. C. Hunt, P. Rudolf, and S. Modesti, Phys. Rev. B **55**, 7882 (1997).
[41] M. Hinterstein, X. Torrelles, R. Felici, J. Rius, M. Huang, S. Fabris, H. Fuess, and M. Pedio, Phys. Rev. B **77**, 153412 (2008).
[42] R. Felici, M. Pedio, F. Borgatti, S. Iannotta, M. Capozi, G. Ciullo, and A. Stierle, Nature Mater. **4**, 688 (2005).